

Temperature-dependent Raman investigation on suspended graphene: Contribution from thermal expansion coefficient mismatch between graphene and substrate



Shibing Tian¹, Yang Yang¹, Zhe Liu, Chao Wang, Ruhao Pan, Changzhi Gu^{**}, Junjie Li^{*}

Beijing National Laboratory for Condensed Matter Physics, Institute of Physics, Chinese Academy of Sciences, Beijing 100190, China

ARTICLE INFO

Article history:

Received 11 January 2016

Received in revised form

11 March 2016

Accepted 19 March 2016

Available online 22 March 2016

ABSTRACT

Dedicated Raman investigation was performed on the graphene suspended on the round holes, compared with graphene supported on Si/SiO₂ substrate, in the temperature range from 173 K to 673 K. We observed an unexpected result that the temperature-dependent Raman frequency shift of suspended graphene was similar as that of supported graphene. This evidenced that the strain caused by thermal expansion coefficient mismatch between graphene and substrate cannot be neglected from suspended graphene. We predicted that the unsupported graphene zone and its surrounding graphene that adhered to substrate should be considered as a whole while studying the thermodynamic properties of this suspended graphene, and thus a semi-quantitative factor was introduced to the estimate the contribution from substrate to the suspended graphene, explaining well this result. Our results suggest that the thermal expansion coefficient mismatch induced strain should be taken into consideration in the study of electronic and transport properties of suspended graphene devices, in which the self-heating effect cannot be eliminated during operation.

© 2016 Elsevier Ltd. All rights reserved.

1. Introduction

Graphene, of two dimensional hexagonal lattice structure, has attracted considerable attention since its first observation in 2004 [1–3]. Owing to its unique structure, various distinct physical properties arise [4–7] and make it a promising candidate for electronic devices [7,8]. Recently, free-standing graphene (FG) received remarkable research interests, because it has exhibited better transport properties than substrate supported graphene (SSG) [4,5,9]. So various electronic devices, such as resonators, electromechanical switch devices, and transistors have been fabricated based on FG [10–12]. It is also reported that the graphene-based force and gas sensors have been fabricated, as the resistance of graphene is very sensitive to the changes of strain [13,14].

It is already reported that the transport properties or band structure can be modified by introducing strain to graphene sheet

[15,16]. Due to the self-heating arising during the operation of graphene-based devices or the changes of ambient temperature, the strain emerges in graphene sheet as a result of the variation of lattice parameters. It has been demonstrated that the thermal expansion coefficient (TEC) of graphene is a key parameter that can modulate the electronic properties of graphene and the performance of graphene-based devices. Therefore, from the application point of view, it is crucial to investigate the TEC of FG as a function of temperature. In recent years, many experimental and theoretical works have been carried out to study the TEC of graphene (α_{gr}). However, these results are still in controversy [17–23]. It was observed by different groups that the sign of TEC changed from negative to positive at different temperatures [17–19]. Mounet and Marzari dedicated a negative α_{gr} based on density functional perturbation theory (DFPT) using a representative of the quasi-harmonic approximation [20]. Magnin et al. found both negative and positive α_{gr} by employing atomistic Monte Carlo (MC) simulations with different potentials [21]. A negative α_{gr} was observed by Yoon et al. using Raman spectroscopy in the range of 200–400 K [22]. Linas and coworkers predicted a positive α_{gr} over room temperature [23]. It is noteworthy that the theoretical calculations were performed on the base of FG. However, most of the

* Corresponding author.

** Corresponding author.

E-mail addresses: czgu@iphy.ac.cn (C. Gu), jjli@iphy.ac.cn (J. Li).

¹ These authors contributed equally.

experimental studies were carried on SSG.

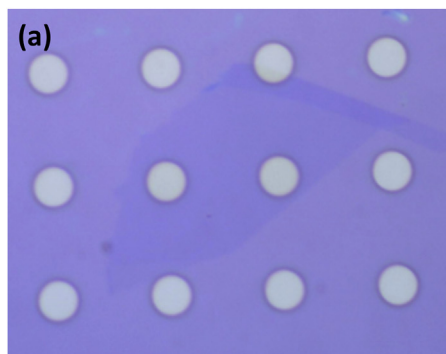
Raman spectroscopy is a powerful technique for investigating the structural and electronic properties of graphene, such as number of layers, stress and doping [24–28], and also Raman spectroscopy has been demonstrated to be a feasible tool to study the thermal behaviors of monolayer graphene [22,23,28–32]. However, all the previous researches were carried on the graphene adhered to substrates. Although some studies have tried to get an insight into the TEC of graphene using substrate corrections methods [22,23], direct Raman investigation on FG is rarely reported so far, to the best of our knowledge.

As we know, however, absolute FG cannot be achievable in the laboratory, which actually exists in the form of suspended graphene (SUG). In the SUG devices, the working or testing zone of the graphene sheet is free of confinement from substrate, while the other part of graphene is adhered to substrate. In this work, a SUG sample was prepared by transferring an exfoliated graphene flake to a Si/SiO₂ substrate with disk-like holes, and was employed as the substitution of FG. A complex Raman study was carried on SUG, compared with graphene on Si/SiO₂ substrate (SSG), in the temperature range from 173 K to 673 K. The Raman peaks for both SUG and SSG shifted linearly to lower frequency positions with increasing temperature. It is noteworthy that the frequency shifts of SUG are very close to that of SSG, which is contrary to our previous hypothesis. This suggests that the TEC mismatch between graphene and SiO₂ substrate play an important role in the frequency shift of SUG as well as SSG. These results indicate that the unsupported graphene zone and its surrounding graphene that adhere to substrate should be considered as a whole while studying the thermodynamic properties of SUG devices. Because the self-heating effect cannot be eliminated during the operation of suspended graphene devices, the strain consequently emerges due to TEC mismatch should be taken into consideration while studying the electronic and transport properties of devices. In addition, the temperature effect should be regarded as a factor when designing force and gas sensors, which are highly sensitive to the changes in the resistance of graphene.

2. Experimental

2.1. Sample preparation

To achieve SUG, a periodic pit array is firstly fabricated on SiO₂ (300 nm)/Si substrate by the UV lithography and reactive ion etching technology, having 5 μm in diameter and 500 nm in depth. Graphene flakes were mechanically exfoliated from natural



graphite onto the pre-patterned SiO₂/Si substrate previously cleaned by oxygen plasma. The single layer graphene is roughly picked out by its purple color (typically on 300 nm thick SiO₂ substrate) from optical microscopy seen in Fig. 1(a), but still need further demonstration by Raman spectroscopy.

2.2. Raman spectroscopy

Raman spectra were collected using a confocal micro-Raman spectrometer (Horiba/Jobin Yvon HR 800). A solid state laser of 532 nm wavelength was used as the excitation source. The laser beam was focused using a 50× long-working distance objective with numeric aperture NA = 0.5, and the spot size was about 1.5 μm. To avoid the local-heating effect, the laser power was controlled to be less than 1 mW on the surface of the heating stage. The sample was placed inside a cryostat cell (Linkam, THMS 600), and the Raman spectra were measured in the temperature range from 173 to 673 K with an interval of 100 K, as shown in Fig.1(b).

3. Results and discussion

Fig. 2 shows the room-temperature Raman spectra of SUG and SSG. One can see that both samples exhibit classic spectral features

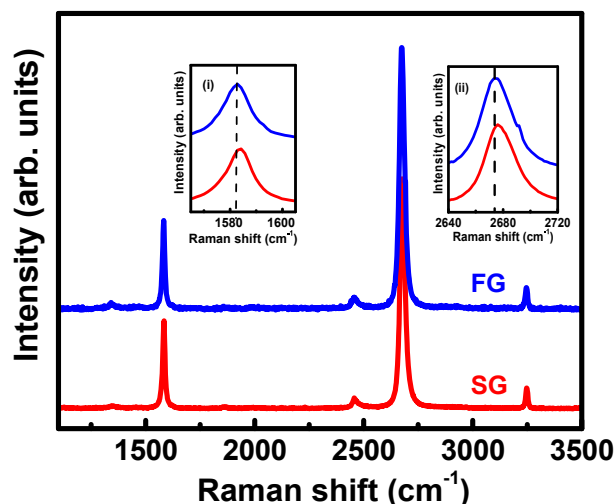


Fig. 2. Room-temperature Raman spectra of SUG and SSG, respectively. The inset figures show zoom-in views of G (i) and 2D (ii) peak areas. (A colour version of this figure can be viewed online.)

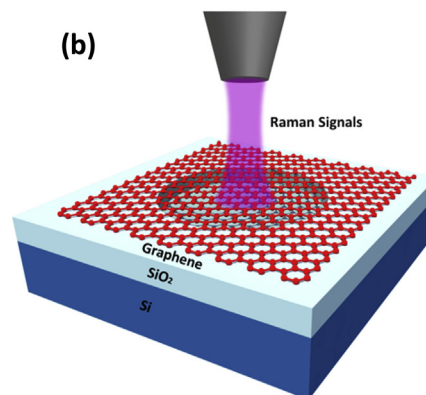


Fig. 1. (a) The optical micrograph of a large exfoliated graphene flake that spanning an array of circular holes with a 5 μm in diameter. (b) Schematic illustration of Raman signals measurement for the graphene suspended on a hole. (A colour version of this figure can be viewed online.)

of monolayer graphene, of which the intensity ratio of 2D band to G band is over two. The two intense peaks at around 1580 and 2680 cm^{-1} are the G and 2D bands, respectively. Besides, two weak peaks at around 2450 and 3250 cm^{-1} are assigned as the T + D and 2D' peaks, respectively [33,34]. It is worthy to note that the frequencies of Raman peaks of SUG are lower than their correspondences of SSG. The downshift of the Raman peaks for SUG compared with SSG was also observed in previous studies [10]. The higher Raman frequencies of SSG would be attributed to the confinement from substrate, although the graphene flake is just attached to the SiO_2 surface by Van der Waals force.

Fig. 3 exhibits the Raman spectra of SUG at selected temperatures, which share the similar behaviors as those of SSG (are not shown here). As shown in Fig. 3, it is notable that all the Raman peaks shift to lower frequencies and broaden with increasing temperature. Moreover, the intensity of 2D peak decreases significantly compared with G band. Similar phenomenon has been reported as well in previous studies [29,30]. As reported in previous publications, the linearly shifts of Raman peaks are associated with thermal expansion of C–C bands [29–31]. Besides, the changes on bandwidth and intensity of 2D band are associated with oxygen induced hole-doping [28]. On the other hand, Apostolov et al. predicted that the electron-phonon coupling also plays an important role in the temperature dependence of G band [35]. As temperature is a homogeneous effect, the graphene lattice will expand or shrink along two axes at the same time with the same variation. As a result, the graphene lattice undertakes a biaxial strain while the lattice changes with temperature. In such a case, the point group remains at D_{6h} , and the G mode does not split (see Fig. 3).

The Raman spectra of SUG and SSG are deconvoluted using Gaussian/Lorentzian mixed function and compared as a function of temperature. One can see that the G band for both SUG and SSG nearly linearly shifts to lower frequency with increasing temperature, as shown in Fig. 4. Following previous reports [28,31], the experimental data can be fitted using a linear function $\omega_t = \omega_0 + \chi T$, where ω_0 and ω_t are the peak frequency at 0 K and selected temperature points, and χ is the slope of the fitting line. The fitting parameters for G and 2D bands are listed in Table 1. The frequency

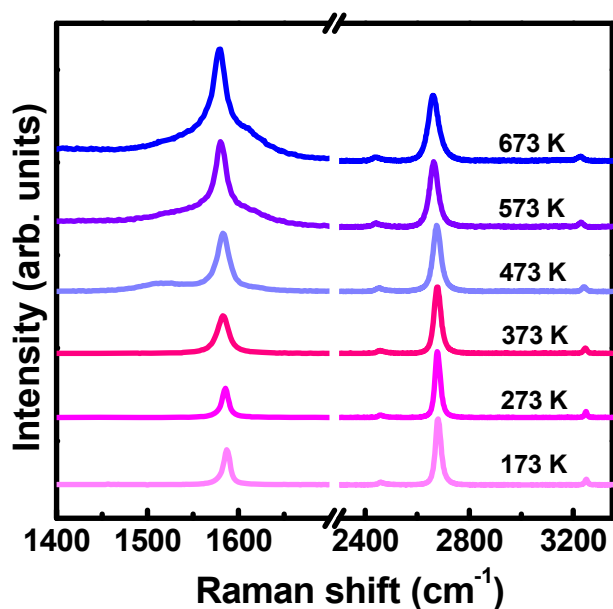


Fig. 3. Raman spectra of SUG at selected temperatures. All spectra are normalized using the intensity of 2D peak. (A colour version of this figure can be viewed online.)

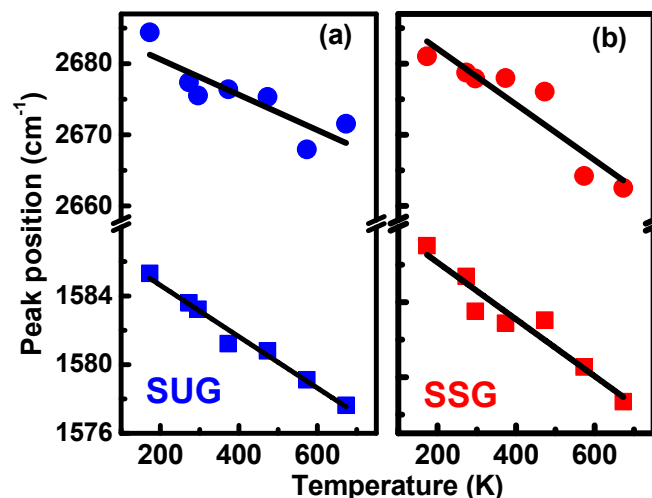


Fig. 4. Temperature-dependent frequencies of G band and 2D of SUG and SSG, respectively. The solid straight lines are the fitted results using a linear function. (A colour version of this figure can be viewed online.)

shift slope of G peak in SUG is $-0.01496 \text{ cm}^{-1} \text{ K}^{-1}$, while the frequency shift slope of SSG is $-0.01517 \text{ cm}^{-1} \text{ K}^{-1}$. The values of slope are in well agreement with previous reports. In contrary to our expectation, the difference of frequency slope between SUG and SSG is very small ($0.00021 \text{ cm}^{-1} \text{ K}^{-1}$). In order to understand this striking phenomenon, further analysis is performed. The temperature behavior of the frequency shift of G peak ($\Delta\omega_G$) is compared between SSG and SUG, after removing the Raman frequency of G peak at $T_0 = 0 \text{ K}$ (ω_{0G}). As shown in Fig. 5(a), the $\Delta\omega_G$ of both SSG and SUG are much smaller than the $\Delta\omega$ of free standing graphene and graphite obtained from DFT calculation. It has been demonstrated by the excellent agreement between theoretical calculation and experimental works that the temperature dependent Raman shift of graphite is determined by the anharmonicity of the C–C interaction [17,36]. The results in Fig. 5(a) imply that the anharmonic property is not the sole contribution to the Raman shift of SUG, although the zone under Raman measurement doesn't attach to substrate.

We can also see in Fig. 5(a) that the $\Delta\omega_G$ of SUG is very close to that of SSG, suggesting the substrate plays an important role in the thermodynamic behavior of free standing graphene suspended on holes. After subtracting $\Delta\omega_G$ of SUG, the residual value of $\Delta\omega_G$ -SSG is shown in Fig. 5(b). It can be seen in Fig. 5(b), the frequency difference gradually decreases from positive value to negative value. This suggested that the thermodynamic of SUG is slightly different from that of SSG. The origin of the discrepancy on frequency shift will be discussed in detail in following section.

It has been reported that the temperature-dependent Raman frequency shift of FG ($\Delta\omega_G(T)$) is commonly attributed to the thermal expansion of the lattice ($\Delta\omega_G^E(T)$) and an anharmonic effect ($\Delta\omega_G^A(T)$) which changes the phonon self-energy [22]. The $\Delta\omega_G(T)$ can be expressed as

$$\Delta\omega_G(T) = \Delta\omega_G^E(T) + \Delta\omega_G^A(T) \quad (1)$$

Table 1
Fitting parameters for the temperature-dependent frequency of G and 2D band.

	$\omega_{0G} (\text{cm}^{-1})$	$\chi_G (\text{cm}^{-1} \text{ K}^{-1})$	$\omega_{02D} (\text{cm}^{-1})$	$\chi_{2D} (\text{cm}^{-1} \text{ K}^{-1})$
FG	1587.6124	-0.01496	2675.53	-0.02484
SG	1589.1534	-0.01517	2677.92	-0.03915

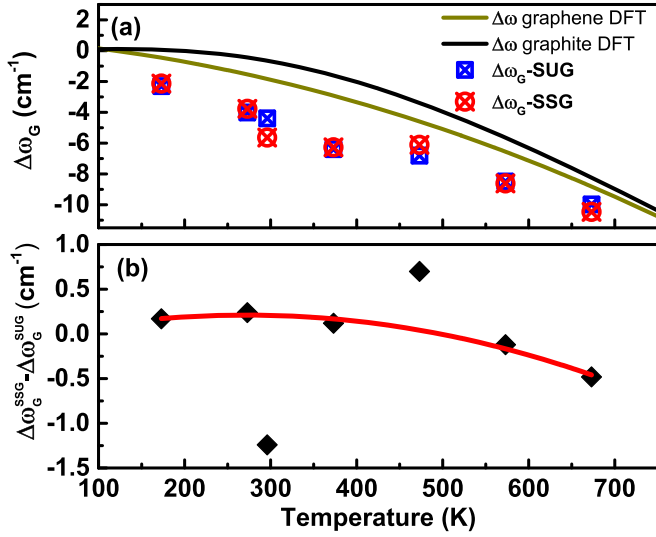


Fig. 5. (a) Raman frequency shifts of G band after removing the frequency at 0 K as a function of temperature. The solid lines represent the Raman shift of graphene and graphite, separately, calculated by Bonini and coworkers from DFT [17]. (b) Frequency differences in $\Delta\omega_G$ between SSG and SUG as a function of temperature. (A colour version of this figure can be viewed online.)

For the graphene pinned on substrates, the thermal behavior of Raman shift of G peak becomes more complex. When temperature varies, both usual thermal effects and strains induced by the TEC mismatch between the substrates and graphene must be taken into consideration. As a result, the frequency shifts of the Raman G band $\Delta\omega_G(T)$ of graphene on a substrate could be written as

$$\Delta\omega_G(T) = \Delta\omega_G^E(T) + \Delta\omega_G^A(T) + \Delta\omega_G^S(T) \quad (2)$$

The contribution to Raman frequency shift from the substrate induced strain ($\Delta\omega_G^S(T)$) can be expressed as

$$\Delta\omega_G^S(T) = \beta \int_{T_0}^T [\alpha_{\text{SiO}_2}(T) - \alpha_{\text{gr}}(T)] dT \quad (3)$$

where β is the biaxial strain coefficient of the G band, $\alpha_{\text{SiO}_2}(T)$ and $\alpha_{\text{gr}}(T)$ are the temperature-dependent TECs of SiO₂ and graphene, respectively. The biaxial strain coefficient β has been known to be $-70 \pm 3 \text{ cm}^{-1}\%$ [25,27]. The value of $\alpha_{\text{SiO}_2}(T)$ can be taken from previous literature [37]. Eq. (3) illustrates the relationship between the Raman frequency shift and TECs of graphene and substrates. Combining Eqs. (1)–(3), we can eliminate the effect from substrate and evaluate the TEC of graphene.

For graphene, several forms of $\alpha_{\text{gr}}(T)$ have been obtained experimentally and theoretically. Bao and coworkers observed that $\alpha_{\text{gr}}(T)$ changes from negative to positive values at around 350 K using scanning electron microscopy [19]. Mounet and Marzari dedicated a negative $\alpha_{\text{gr}}(T)$ based DFPT calculation [20]. Based on this model, Yoon et al. observed a negative α up to 400 K using Raman spectroscopy [22]. Lindsay and Brodido predicted a positive $\alpha_{\text{gr}}(T)$ using DFT calculation [38] with a reparametrization of the Tersoff bond-order potential [38]. Linas et al. suggested a positive $\alpha_{\text{gr}}(T)$ above room temperature by substrate correction with Lindsay-Brodido model [23]. Therefore, in this work, different $\alpha_{\text{gr}}(T)$ are tried and compared in order to find the most suitable form of $\alpha_{\text{gr}}(T)$, as shown in Fig. 6. The TECs from Lindsay-Brodido model $\alpha_{\text{LB}}(T)$ and Mounet-Marza model $\alpha_{\text{M}}(T)$ are employed in Eq. (3), respectively, for integrating over temperature. Then, the frequency

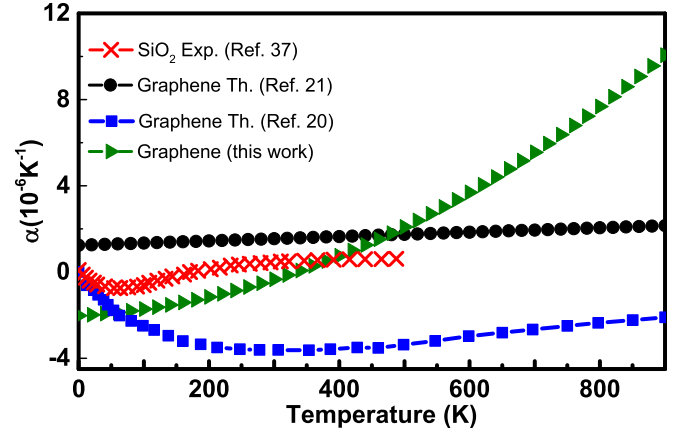


Fig. 6. Temperature dependence of the TECs α of SiO₂ (red crosses), experimentally obtained TECs α of graphene in this work (green triangles), and theoretical in-plane coefficients of graphene obtained by Mounet and Marzari using DFPT calculation (blue squares) and from Lindsay-Brodido using DFT calculation for graphene (black circles). (A colour version of this figure can be viewed online.)

shifts of SSG in our work corrected by removing the substrate effect with $\alpha_{\text{LB}}(T)$ and $\alpha_{\text{M}}(T)$, respectively, are plotted in Fig. 7. As reported previously [22,23], the theoretical Raman frequency shift of free-standing graphene calculated by Bonini and coworkers [17] using density-functional theory (DFT) calculations under appropriate anharmonic expansions is adapted as reference. As shown in Fig. 7, large discrepancies between the results corrected with $\alpha_{\text{LB}}(T)$ and $\alpha_{\text{M}}(T)$ models and the DFT reference data are observed, which suggest a new form of α_{gr} should be evolved into our work for the substrate correction.

And thus, the expression of $\Delta\omega_G^S(T)$ Eq. (3) could be transformed as following

$$\Delta\omega_G^S(T) = \beta \int_{T_0}^T \alpha_{\text{SiO}_2}(T) dT - \beta \int_{T_0}^T \alpha_{\text{gr}}(T) dT \quad (4)$$

As shown in Fig. 6, α_{SiO_2} is already known, so that the

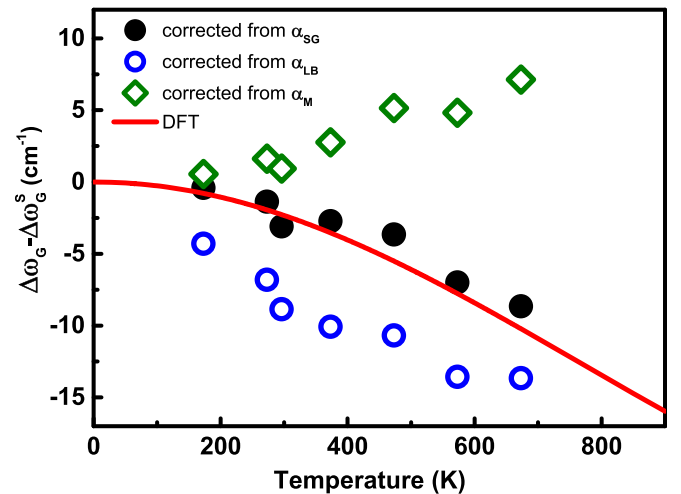


Fig. 7. Raman frequency shift of G band corrected from the substrate mismatch contribution using different model TEC α_{gr} : the α_{SG} derive from our experiment data (α_{SG} , solid circles), the Mounet-Marzari model (α_{M} , open squares) and the Lindsay-Brodido model (α_{LB} , open circles) as a function of temperature. The solid line shows the Raman shift calculated by Bonini and coworkers from DFT [17]. (A colour version of this figure can be viewed online.)

contribution from the TEC of SiO₂ can be obtained by integration. By adopting the DFT reference data as pure frequency shifts $\Delta\omega_G(T) - \Delta\omega_G^S(T)$ into our work, the temperature-dependent of $\alpha_{gr}(T)$ can be derived from Eqs. (2) and (4). The calculated $\alpha_{gr}(T)$ is nominated as $\alpha_{SG}(T)$, which can be expressed using a quadratic function $\alpha_{SG}(T) = -2.02363 + 0.00173T + 1.299 \times 10^{-5}T$. Different forms of α_{gr} have been obtained by using different semi-empirical potentials in Monte Carlo simulations [21]. The temperature behavior of the $\alpha_{SG}(T)$ in our work is similar as those obtained by Teroff and LCBOB potentials. On the other hand, a linearly varied $\alpha_{gr}(T)$ obtained using Lindsay-Broido potential (black dots in Fig. 6) was employed to explain the temperature dependent Raman shifts of graphene on SiN/Si substrate [23]. As shown in Fig. 6, the sign of $\alpha_{SG}(T)$ changes from negative to positive at around 400 K, which is the same as that predicted in Yoon's work [22]. In addition, one can see that α_{SG} is around $-0.4 \times 10^{-6} \text{ K}^{-1}$ at room temperature, which is between the values those used in Yoon's ($-8.0 \times 10^{-6} \text{ K}^{-1}$) and Linas's ($1.55 \times 10^{-6} \text{ K}^{-1}$) works [22,23]. As shown in Fig. 7, the values of $\Delta\omega_G(T) - \Delta\omega_G^S(T)$ in our work show well agreement with DFT data after introducing the obtained $\alpha_{SG}(T)$ into the calculation of pure frequency shift.

On the other hand, there is still a certain discrepancy on frequency shift between SUG and SSG, as presented in Fig. 5(b). In order to explain this phenomenon, the preparation progress of SUG should be taken into consideration. In this work, only the graphene above the hole is unsupported, but most part of the SUG sheet is adhered to SiO₂ layer. Although there is no work directly reported the adhesive force from pinned graphene to the suspended graphene, the adhesive force from pinned graphene exclusively exists and has been predicted in the studies of the elastic properties and blister of suspended graphene [6,39]. Therefore, the contribution from the adhered graphene should be taken into consideration in the investigation of the temperature behavior of SUG. While temperature varies, the strains induced by the TEC mismatch between the substrates and graphene will be suppressed on graphene area that is pinned on SiO₂ area, performing the same as what did in SSG. Obviously, the graphene suspended over the hole is strongly connected with the pinned graphene area by strong covalent bonds interactions. While the temperature changing, the Raman frequency shift of the SUG is definitely modulated by the graphene section that is pinned on substrate. When evaluating the thermodynamic of SUG, the graphene sheet should be taken as a whole, including unsupported graphene over the hole and the graphene section pinned on substrate. As the graphene flake is continuous, the contribution from α_{gr} doesn't change in Eq. (4). Only the part related with α_{SiO_2} needs to be revised because of holes on the substrate. Thus, the expression of $\Delta\omega_G^S(T)$ for SUG could be written as following

$$\Delta\omega_G^S(T) = \beta \cdot R_{rel} \int_{T_0}^T \alpha_{SiO_2}(T) dT - \beta \int_{T_0}^T \alpha_{gr}(T) dT \quad (5)$$

where R_{rel} implies the relative contribution of SiO₂ substrate to SUG. Approximately, we tried to represent R_{rel} using the area ratio of the SSG to the whole graphene flake. As shown in Fig. 1, the periodicity of the holes is $12 \mu\text{m} \times 12 \mu\text{m}$, while the diameter of the disc-like hole is $5 \mu\text{m}$. Hence, the estimated the relative contribution from SiO₂ is $R_{rel} = 0.8636$ for the SUG in our work. Introducing the $\Delta\omega_G(T) - \Delta\omega_G^S(T)$ obtained from SSG (shown in Fig. 7) into Eq. (5), the contribution from SiO₂ into the frequency shift of SUG is deduced, and its ratio to that of SSG plotted in Fig. 8. One can see that except 473 K, the values of ratio are less than 1 at other temperature points. The abnormal at 473 K may be due to the errors in

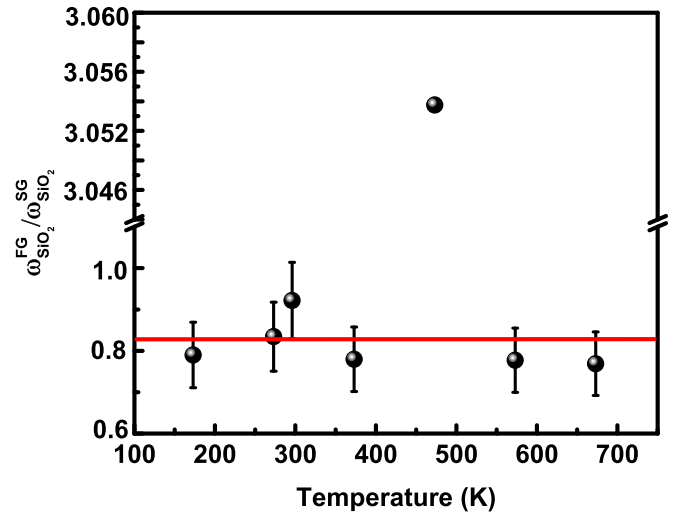


Fig. 8. The ratio of the frequency shift arising from SiO₂ substrate for SUG to that for SSG. The red line is a guide to the eye. (A colour version of this figure can be viewed online.)

the measurements. The lattice symmetry and surface roughness of substrate may also effect the evaluation of contribution of TEC mismatch in the Raman shift of graphene. As we know, the single crystal transition metal dichalcogenides (TMDs), such as MoS₂, WS₂, which have similar lattice symmetry and atomically flat surface as graphene. Therefore, cleaved single crystal TMDs would be good candidate of supporting substrates which could reduce the errors in future measurement. As indicated by the red line in Fig. 8, the average ratio is 0.8119 over the temperature range, which is very close to the calculated relative contribution factor R_{rel} . Our prediction that the unsupported and supported graphene areas should be considered as whole is reasonable. Of course, the adhesive graphene should affect the thermal expansion of SUG zone in a certain distance, so-called coherent length. Out of this length, the substrate contribution to SUG could be neglected. Additional experimental and theoretical works are needed to clarify the coherent length in SUG, which is outside the scope of this work.

The results shown in Fig. 8 imply that with temperature changing, the strain arise from SUG due to TEC mismatch as well as that did in SSG. This would be helpful for understanding the electronic and transport behaviors of SUG based devices. It has been reported that the resistance of graphene will be modulated by involving strain in graphene sheet [15,25]. As we know, self-heating or joule heating is a serious side effect which cannot be eliminated during the operation of graphene transistors [40]. In this case, with increasing temperature of the device, the strain will be suppressed in SUG by the TEC mismatch between graphene and substrate. The electronic and transport properties of SUG devices will be modulated as a result. In addition, the changes in the ambient temperature can also introduce the strain into the graphene, which should be taken into account during designing SUG devices, especially for high sensitivity force and gas sensors at low and high temperature conditions.

4. Conclusion

In this work, comprehensive Raman study was carried respectively on supported and suspended graphene in the temperature range from 173 K to 673 K. Like SSG, the temperature dependent of frequency shift of the SUG is significantly affected by the thermal expansion coefficient mismatch between graphene and substrate.

This phenomenon was well explained by a scheme that the unsupported graphene and its surrounding graphene adhered to substrate are considered as a whole. A semi-quantitative factor R_{rel} , obtained by the area ratio of the graphene adhered to substrate to the whole SUG, was introduced to estimating the relative contribution of substrate to SUG. Our results suggest that as well as SSG devices, the TEC mismatch induced strain plays an important role in the transport properties of SUG electronic devices. In addition, it implies that the changes in the ambient temperature should be taken into consideration while designing SUG-based force and gas sensors.

Acknowledgment

This work was supported by the National Natural Science Foundation of China (Grant Nos. 91323304, 11174362, 91023041, 61390503, 51272278, 11504414).

References

- [1] K.S. Novoselov, A.K. Geim, S.V. Morozov, D. Jiang, Y. Zhang, S.V. Dubonos, et al., Electric field effect in atomically thin carbon films, *Science* 306 (2004) 666–669.
- [2] K.S. Novoselov, D. Jiang, F. Schedin, T.J. Booth, V.V. Khotkevich, S.V. Morozov, et al., Two-dimensional atomic crystals, *Proc. Natl. Acad. Sci. U. S. A.* 102 (2005) 10451–10453.
- [3] A.K. Geim, K.S. Novoselov, The rise of graphene, *Nat. Mater* 6 (2007) 183–191.
- [4] X. Du, I. Skachko, A. Barker, E.Y. Andrei, Approaching ballistic transport in suspended graphene, *Nat. Nanotechnol.* 3 (2008) 491–495.
- [5] J.H. Seol, I. Jo, A.L. Moore, L. Lindsay, Z.H. Aitken, M.T. Pettes, et al., Two-dimensional phonon transport in supported graphene, *Science* 328 (2010) 213–216.
- [6] C. Lee, X. Wei, J.W. Kysar, J. Hone, Measurement of the elastic properties and intrinsic strength of monolayer graphene, *Science* 321 (2008) 385–388.
- [7] K.S. Novoselov, Z. Jiang, Y. Zhang, S.V. Morozov, H.L. Stormer, U. Zeitler, et al., Room-temperature quantum hall effect in graphene, *Science* 315 (2007) 1379.
- [8] K.I. Bolotin, F. Ghahari, M.D. Shulman, H.L. Stormer, P. Kim, Observation of the fractional quantum Hall effect in graphene, *Nature* 462 (2009) 196–199.
- [9] K.I. Bolotin, K.J. Sikes, Z. Jiang, M. Klima, G. Fudenberg, J. Hone, et al., Ultrahigh electron mobility in suspended graphene, *Solid State Commun.* 146 (2008) 351–355.
- [10] S. Shivaraman, R.A. Barton, X. Yu, J. Alden, L. Herman, M. Chandrashekar, et al., Free-standing epitaxial graphene, *Nano Lett.* 9 (2009) 3100–3105.
- [11] Z. Shi, H. Lu, L. Zhang, R. Yang, Y. Wang, D. Liu, H. Guo, et al., Studies of graphene-based nanoelectromechanical switches, *Nano Res.* 5 (2012) 82–87.
- [12] J. Lee, L. Tao, Y. Hao, R.S. Ruoff, D. Akinwande, Embedded-gate graphene transistors for high-mobility detachable flexible nanoelectronics, *Appl. Phys. Lett.* 100 (2012) 152104–152114.
- [13] M. Huang, T.A. Pascal, H. Kim, W.A. Goddard, J.R. Greer, Electronic-mechanical coupling in graphene from in situ nanoindentation experiments and multi-scale atomistic simulations, *Nano Lett.* 11 (2011) 1241–1246.
- [14] I. Iezhokin, P. Offermans, S.H. Brongersma, A.J.M. Giesbers, C.F.J. Flipse, High sensitive quasi freestanding epitaxial graphene gas sensor on 6H-SiC, *Appl. Phys. Lett.* 103 (2013) 053514–053515.
- [15] E.V. Castro, H. Ochoa, M.I. Katsnelson, R.V. Gorbachev, D.C. Elias, K.S. Novoselov, et al., Limits on charge carrier mobility in suspended graphene due to flexural phonons, *Phys. Rev. Lett.* 105 (2010) 266601–266604.
- [16] K. Xu, K. Wang, W. Zhao, W. Bao, E. Liu, Y. Ren, et al., The positive piezoconductive effect in graphene, *Nat. Commun.* 6 (2014) 8119–8126.
- [17] N. Bonini, M. Lazzeri, N. Marzari, F. Mauri, Phonon anharmonicities in graphite and graphene, *Phys. Rev. Lett.* 99 (2007) 176802–176804.
- [18] J.H. Los, L. Chiringhelli, E. Meijer, A. Fasolino, Finite. Temperature lattice properties of graphene beyond the quasiharmonic approximation, *Phys. Rev. B* (2005) 72, 214102–14.
- [19] W. Bao, F. Miao, Z. Chen, H. Zhang, W. Jang, C. Dames, et al., Controlled ripple texturing of suspended graphene and ultrathin graphite membranes, *Nat. Nanotechnol.* 4 (2009) 562–566.
- [20] N. Mounet, N. Marzari, First-principles determination of the structural, vibrational and thermodynamic properties of diamond, graphite, and derivatives, *Phys. Rev. B* (2005) 71, 205214–14.
- [21] Y. Magnin, G.D. Förster, F. Rabilloud, F. Calvo, A. Zappelli, C. Bichara, Thermal expansion of free-standing graphene: Benchmarking semi-empirical potentials, *J. Phys. Condens Matter* 26 (2014) 185401–185410.
- [22] D. Yoon, Y. Son, H. Cheong, Negative thermal expansion coefficient of graphene measured by Raman spectroscopy, *Nano Lett.* 11 (2011) 3227–3231.
- [23] S. Linas, Y. Magnin, B. Poinso, O. Boisron, G.D. Förster, V. Martinez, et al., Interplay between Raman shift and thermal expansion in graphene: temperature-dependent measurements and analysis of substrate corrections, *Phys. Rev. B* 91 (2015) 075426–075435.
- [24] A.C. Ferrari, J.C. Meyer, V. Scardaci, C. Casiraghi, M. Lazzeri, F. Mauri, et al., Raman spectrum of graphene and graphene layers, *Phys. Rev. Lett.* 97 (2006) 187401–187404.
- [25] Z.H. Ni, T. Yu, Y.H. Lu, Y.Y. Wang, Y.P. Feng, Z.X. Shen, Uniaxial strain on graphene: Raman spectroscopy study and band-gap opening, *ACS Nano* 2 (2008) 2301–2305.
- [26] T.M.G. Mohiuddin, A. Lombardo, R.R. Nair, A. Bonetti, G. Savini, R. Jalil, et al., Uniaxial strain in graphene by Raman spectroscopy: G peak splitting, Grüneisen parameters, and sample orientation, *Phys. Rev. B* (2009) 79, 205433–8.
- [27] D. Yoon, Y.W. Son, H. Cheong, Strain-dependent splitting of the double-resonance Raman scattering band in graphene, *Phys. Rev. Lett.* 106 (2011) 155502–155504.
- [28] H. Zhou, C. Qiu, F. Yu, H. Yang, M. Chen, L. Hu, et al., Raman scattering of monolayer graphene: the temperature and oxygen doping effects, *J. Phys. D. Appl. Phys.* 44 (2011) 185404–185406.
- [29] J. Lin, L. Guo, Q. Huang, Y. Jia, K. Li, X. Lai, et al., Anharmonic phonon effects in Raman spectra of unsupported vertical graphene sheets, *Phys. Rev. B* 83 (2011) 125430–125437.
- [30] S. Berciaud, Y.M. Han, K.F. Mak, L.E. Brus, P. Kim, T.F. Heinz, Electron and optical phonon temperatures in electrically biased graphene, *Phys. Rev. Lett.* 104 (2010) 227401–227404.
- [31] I. Calizo, A.A. Balandin, W. Bao, F. Miao, C.N. Lau, Temperature dependence of the Raman spectra of graphene and graphene multilayers, *Nano Lett.* 7 (9) (2007) 2645–2649.
- [32] K.T. Nguyen, D. Abdula, C.L. Tsai, M. Shim, Temperature and gate voltage dependent Raman spectra of single-layer graphene, *ACS Nano* 5 (2011) 5273–5279.
- [33] P.H. Tan, Y.M. Deng, Q. Zhao, Temperature-dependent Raman spectra and anomalous Raman phenomenon of highly oriented pyrolytic graphite, *Phys. Rev. B* 58 (1998) 5435–5439.
- [34] Y. Kawashima, G. Katagiri, Fundamentals, overtones, and combinations in the Raman spectrum of graphite, *Phys. Rev. B* 52 (1995) 10053–10059.
- [35] A.T. Apostolov, I.N. Apostolova, J.M. Wesselinowa, Temperature and layer number dependence of the G and 2D phonon energy and damping in graphene, *J. Phys. Condens Matter* 24 (2012) 235401–235409.
- [36] P. Giura, N. Bonini, G. Creff, J.B. Brubach, P. Roy, M. Lazzeri, Temperature evolution of infrared- and Raman-active phonons in graphite, *Phys. Rev. B* 86 (2012), 121404(R)–4.
- [37] NIST, Standard Reference Material 739 Certificate, 1991.
- [38] L. Lindsay, D.A. Broido, Optimized Tersoff and Brenner empirical potential parameters for lattice dynamics and phonon thermal transport in carbon nanotubes and graphene, *Phys. Rev. B* 81 (2010) 205441–205446.
- [39] D. Metten, F. Federspiel, M. Romeo, S. Berciaud, All-optical blister test of suspended graphene using micro-Raman spectroscopy, *Phys. Rev. Appl.* 2 (2014) 054008–054011.
- [40] T.S. Pan, M. Gao, Z.L. Huang, Y. Zhang, X. Feng, Y. Lin, The impact of the thermal conductivity of a dielectric layer on the self-heating effect of a graphene transistor, *Nanoscale* 7 (2015) 13561–13567.